*29th EPS Conference on Plasma Phys. and Contr. Fusion Montreux, 17-21 June 2002 ECA Vol. **26B**, P-5.029 (2002)*

Non-Diffusive Transport Phenomena in TJ-II

B. Ph. van Milligen, F. Castejón, F. Tabarés, E. Ascasíbar, T. Estrada, L. García[1], I. García-Cortés, J. Herranz, C. Hidalgo, J.A. Jimenez, E. de la Luna, F. Medina, M. Ochando, I. Pastor, M. A. Pedrosa, A. Petrov[2], R. Sánchez[1], K. Sarksian[2], N. Skvortsova[2], D. Tafalla

Laboratorio Nacional de Fusión por Confinamiento Magnético,
Asociación Euratom-CIEMAT, 28040 Madrid, Spain.
[1] Universidad Carlos III, 28911 Madrid, Spain
[2] General Physics Institute, Russ. Acad. of Sciences, ul. Vavilova 38, Moscow, 199911 Russia

Introduction – The radial propagation of perturbations is an important tool for probing transport properties in a fusion plasma. Indeed, the propagation of cold pulses, induced by either deliberate or spontaneous edge cooling, has been studied in many devices (e.g. JET [1, 2, 3], TFTR [4], TEXT [5], RTP [6, 7], ASDEX [8] and W7-AS [9]). The analysis of such pulses has led to the conclusion that often this phenomenon is not in agreement with standard diffusive model predictions. In this paper, an analysis of the propagation of cold and heat pulses is presented and it is found that this phenomenon is likewise difficult to reconcile with a simple diffusive transport model in a stellarator like TJ-II.

Experimental set-up – The TJ-II stellarator [10] is a low-shear Heliac having 4 periods, $B_0 < 1.2$ T, $R = 1.5$ m and $a \leq 0.22$ m. Plasmas are bean-shaped. The configuration used in this paper is denoted by "100_40_63", a standard TJ-II configuration with $\iota(a)/2\pi = 1.61$ and $\iota(0)/2\pi = 1.51$. The plasmas were heated by the Electron Cyclotron Heating system, using one gyrotron with a frequency $f = 53.2$ GHz and with power $P \leq 300$ kW (2^{nd} harmonic, extraordinary mode). The wall was metallic. A multi-channel heterodyne radiometer [11], provided simultaneous measurement of the electron temperature at 8 positions on the high field side, with good temporal resolution and radial resolution of about 1 cm. The radiometer is absolutely calibrated, and the accuracy is reflected by the good agreement found between the Thomson Scattering and ECE temperatures. The high-resolution single-shot Thomson scattering system measures electron temperatures in the range from 50 eV to 4 keV, with a spatial resolution of 2.25 mm and with about 280 data points along the line of sight [12].

Cold-pulse experiments – Cold pulses were generated using fast nitrogen injection. Nitrogen remains confined mainly in the edge region of the plasma [13], so that the initial perturbation is an edge effect, and the penetration of high-Z material into the plasma is small.

The response of ECE radiometer signals is shown in Fig. 1. Each temperature trace is initially nearly constant, and then experiences a sudden drop followed by a slow recovery. The line-average density increases slightly after injection of the cold pulse, but typically the perturbation is less than about 7%. The response of the H_α detector is shown in Fig. 2. The detector picks up the radiation by molecular nitrogen (654 nm, seen through an H_α interference filter) and the signal amplitude is thus indicative of the amount of nitrogen

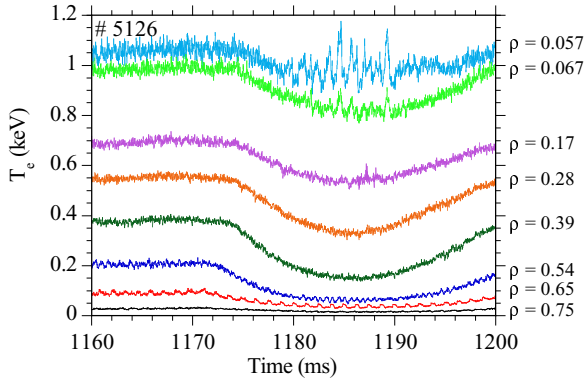

Fig 1 - ECE electron temperature traces for discharge 5126.

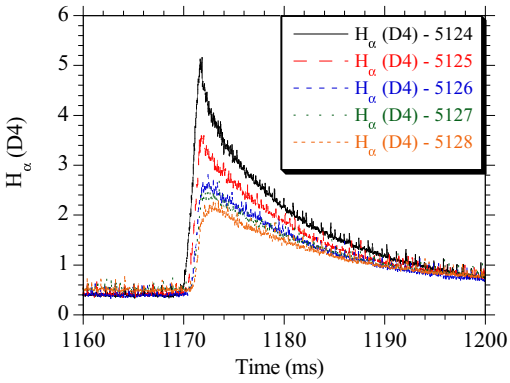

Fig. 2 - Signal of the H_α detector.

injected. The time of injection is marked by the steep flank of this trace. The electron temperature was also measured at the limiter (at ρ =1) by Langmuir probes. It was seen to drop sharply from approximately 18 to 10 eV, about 1 ms after the rising flank of the nitrogen radiation. Thus, the nitrogen radiation peak must be located inside the last closed flux surface (LCFS), and the cold pulse propagates both in- and outwards from that position. The radiation peak is estimated to be near ρ = 0.8. Likewise, the reciprocating Langmuir probes measured the floating potential and the ion saturation current during the cold pulse (at $\rho \approx 0.8$). The root-mean-square (RMS) variation of the floating potential, a measure for the electrostatic turbulence level, is reduced by a factor of three during the cold pulse, and correlates well with the temperature drop. This is probably related to the reduction of the local edge pressure gradient. Furthermore, the Soft X-Ray tomography system also detected the effects of the cold pulse. Repetition of the experiments with a boronised wall gave less clear results due to changes in particle recyling, limiting the amplitude of the nitrogen puff.

Spontaneous heat pulses – In the same set of discharges, a central instability caused short-lived spikes in the central ECE channel (Fig. 3). These temperature spikes then propagate outwards. A cross-correlation analysis between ECE channels reveals the average propagation speed though time delays at known channel separations (Fig. 4 and see below).

Analysis – We define the cold pulse front by the time instant the local electron temperature changes sharply. At the time of arrival of the pulse front, the plasma parameters are unaffected by the perturbation, and thus this time of arrival is a probe of the transport properties of the *unperturbed* plasma. Fig. 5 shows the results of this analysis for this series of discharges. The propagation speed is v = 10–20 m/s in the outer half of the plasma ($\rho \geq$ 0.4), whereas it speeds up to v = 50–80 m/s in the central part ($\rho < 0.4$). The velocity of the outward heat pulses, observed in these *same* discharges prior to the injection of Nitrogen, is around 115 m/s, i.e. comparable to the central cold pulse propagation velocity. The frequency analysis of a Mirnov coil signal (Fig. 6) shows that a 43 kHz MHD mode is triggered at the time the cold pulse arrives at $\rho \approx 0.3$–0.4, as deduced from Fig. 5. Most likely, this mode is

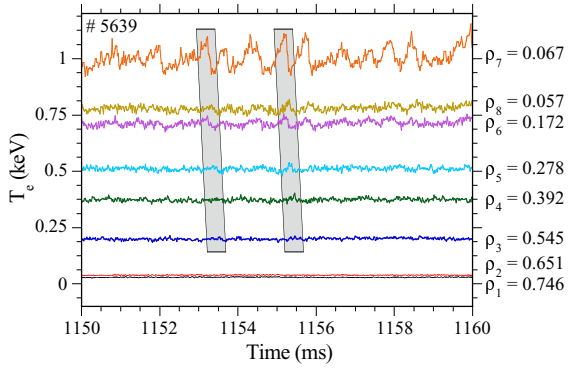

Fig 3 - ECE electron temperature traces showing the propagation of heat pulses.

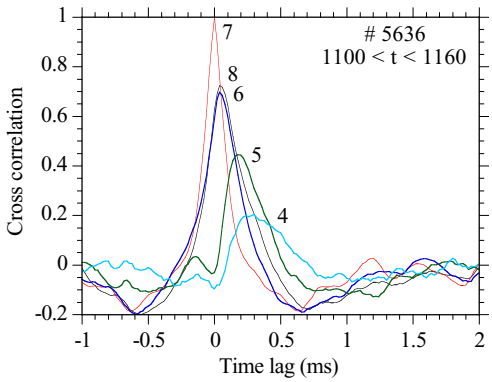

Fig. 4 - Cross-correlation between ECE channels.

an n/m = 3/2 mode. The central value of ι of the vacuum field configuration, ι =1.51, is just above this value, but the small net plasma current measured by a Rogowski coil ($I_p \approx -0.2$ kA), moves the ι = 3/2 rational surface to approximately $\rho \approx 0.3$, consistent with the observation. The island width must be less than the channel separation of the ECE diagnostic,

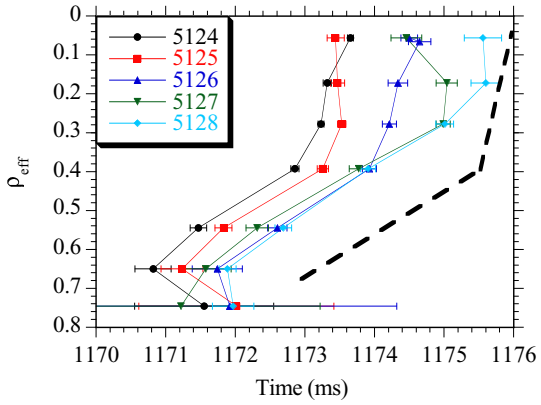

Fig 5 - Time of arrival of the cold pulse front, seen with the ECE diagnostic. The dashed line corresponds to propagation at 10 m/s for $\rho > 0.4$ and at 80 m/s for $\rho < 0.4$.

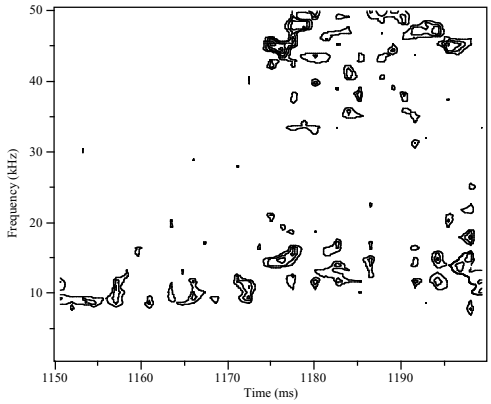

Fig 6 - Plot of the spectrum of a Mirnov coil (shot 5127). A 43 kHz mode is activated at t ≈ 1173 ms, when the cold pulse front arrives at ρ = 0.3–0.4.

as no significant flattening is observed. Likewise, in other but similar discharges, high-resolution Thomson scattering profiles are available before and after the cold pulse, showing an island-like structure in the second case, having a width of around 1 cm in the mid-plane at $\phi = 45^o$. Likewise, the 2-mm scattering diagnostic, sensitive to wavelengths of 3- and 6-cm^{-1}, observed a sharp change in the detected signal, coincident with the time instant the cold pulse front reached its measurement location (at $\rho = 0.6$).

Interpretation – The propagation of the cold pulse front reported in this paper is non-diffusive for the following reasons: (1) The propagation velocity is constant over sections of the plasma, and even accelerates towards the centre, while diffusive propagation would slow down faster than $v \propto 1/\sqrt{t}$, since the heat diffusivity χ is known to be smaller in the centre than in the edge: 2 (centre) < χ < 4 (edge) m^2/s [14]. (2) The pulse front remains sharp in

time, while diffusion would smear the front out. (3) A fit of the data to a diffusive model that includes a pinch term fails to reproduce the observed behaviour, similar to what has been reported elsewhere [5]. (4) Simultaneous inward and outward propagation is difficult to reconcile with a pinch term. The observation of non-diffusive (or "ballistic") propagation of cold pulses is in accord with observations on other devices: e.g. TEXT ($v \approx$ 10-20 m/s in the edge region) [5], RTP ($v \approx$ 500 m/s) [6], and JET ($v \approx$ 160 m/s) [3]. Only strongly non-linear and non-local modifications to the diffusive transport model would be able to model the observations. This road has been explored in several of the cited publications, but the physical justification of this approach remains obscure.

Qualitatively, the pulse propagation behaviour observed and reported here is very similar to the pulse propagation seen in a simulation of resistive pressure-gradient driven turbulence in cylindrical geometry [15]. Here, the propagation velocity is determined by the mode growth rates and the width of the modes, since the propagation involves the successive destabilisation of modes on adjacent rational surfaces ($v \approx \gamma W$, [16]). The resistive time is $\tau_R = a^2 \cdot \mu_0 / \eta$ = 100–200 ms and the resistive velocity is a / τ_R = 1–2 m/s. The observation made in [15] that the propagation velocity should be about one order of magnitude faster than this is in rough agreement with the measurements. A more precise calculation based on [17] and the (smoothed) Thomson scattering pressure profiles reveals that this model not only reproduces the propagation velocity within a factor of 2–3, but even reproduces the central acceleration, mainly related to the gradient of the pressure profile that increases toward the centre. Thus, the most likely explanation for the observed propagation of the cold pulse front is the sequential triggering of pressure-gradient driven modes, in an avalanche-like fashion.

References

[1] JET Team, Proc. 15th IAEA Conf. Seville **1** (1994) 307

[2] Galli, P., *et al.*, Nucl. Fusion **38** (1998) 1355

[3] Sarazin, Y., *et al.*, 27th EPS Conference, Budapest, June 2000, ECA Vol. **24B** (2000) 253

[4] Kissick, M.W., *et al.*, Nucl. Fusion **36** (1996) 1691

[5] Gentle, K. W., *et al.*, Phys. Plasmas **4** (1997) 3599

[6] Galli, P., *et al.*, Nucl. Fusion **39** (1999) 1355

[7] Mantica, P., *et al.*, Phys. Rev. Lett. **82** (1999) 5048

[8] Ryter, F., *et al.*, Nucl. Fusion **40** (2000) 1917

[9] Koponen, J.P.T., *et al.,* Nucl. Fusion **40** (2000) 365

[10] Alejaldre, C., *et al.*, Plasma Phys. Control. Fusion **41** (1999) A539

[11] de la Luna, E., *et al.*, Rev. Sci. Instrum. **72** (1) (2001) 379

[12] Barth, C.J., *et al.*, Rev. Sci. Instrum. **70** (1999) 763

[13] Hildebrandt, D., *et al.*, Journal of Nuclear Materials **241-243** (1997) 950; Monier-Garbet, P., *et al.,* Journal of Nuclear Materials **290-293** (2001) 925

[14] García-Cortés, I., *et al.*, Nucl. Fusion **40** (2000) 1867; F. Castejón, F., *et al.*, Nucl. Fusion **42** (2002) 271

[15] Carreras, B.A., *et al.*, Phys. Plasmas **3** (8), 1996, p. 2903

[16] Diamond, P.H., et al., Phys. Plasmas 2 (1995) 3685

[17] García, L., *et al.*, Phys. of Plasmas **6** (1999) 107